Top-quark signatures at the Fermilab Tevatron collider

H. Baer
Physics Department, Florida State University, Tallahassee, Florida 32303

V. Barger
Physics Department, University of Wisconsin, Madison, Wisconsin 53706

H. Goldberg
Physics Department, Northeastern University, Boston, Massachusetts 02115

R. J. N. Phillips
Rutherford Appleton Laboratory, Chilton, Didcot, Oxon, England
(Received 10 December 1987)

Calculations are presented for the experimental signals arising from top-quark production in $p\bar{p}$ collisions with semileptonic top decay, for the center-of-mass energy $\sqrt{s}=2$ TeV available at the Fermilab Tevatron. Both the strong production of $t\bar{t}$ pairs via QCD and the electroweak channels $W^+\to t\bar{b}$, $W^-\to b\bar{t}$ are considered, including gluon bremsstrahlung effects and complete cascade decays of heavy quarks. To separate the t signal from $b\bar{b}$, $c\bar{c}$, $b\bar{b}b\bar{b}$, W, Z, and other backgrounds, we require events containing an isolated lepton along with n jets ($n\geq 2$). The top mass may be determined by the three-jet invariant mass, or a transverse mass formed from the lepton, third hardest jet, and missing p_T. For $m_t\lesssim 80$ GeV, confirmation of this signal may be obtained from observation of events containing two isolated leptons at high p_T. From these results, we expect the upcoming run of the Fermilab Tevatron collider to be able to probe t masses up to $m_t=100$ GeV, assuming sufficient detector resolution.

I. INTRODUCTION

The top quark t is an essential part of the standard electroweak model where it is required to cancel the triangle anomalies,[1] to explain the suppression of neutral-current $B\to e^+e^-X$ decay modes[2] and to explain the observed value of the $e^+e^-\to b\bar{b}$ forward-backward jet asymmetry.[3] The top-quark mass m_t is an important parameter: overall consistency including radiative corrections[4] requires $m_t<168$ GeV. Arguments[5] based on Γ_Z/Γ_W data suggest $m_t\lesssim 70$ GeV if there are only three fermion generations while arguments[6] based on B^0-$\bar{B}^0$ oscillation data suggest $m_t\gtrsim 50$ GeV. Future precise measurements of weak-boson properties[7] and decays[8] such as $B\to K_\gamma$ may also constrain m_t. The fact that top production has not yet been identified experimentally can be attributed to a large mass value. The latest direct mass limits are $m_t>26$ GeV from the absence of an $e^+e^-\to t\bar{t}$ signal at the KEK collider TRISTAN (Ref. 9) and $m_t>44$–56 GeV from the absence of top signals at the CERN $p\bar{p}$ collider[10] (where the more stringent limit depends on EUROJET t-quark production cross sections). It is therefore quite possible that the mass is too high for $e^+e^-\to t\bar{t}$ production to occur at the SLAC Linear Collider (SLC) or the CERN collider LEP I, and that the only way for the top quark to be produced and identified experimentally in the near future is via $p\bar{p}$ collisions at the CERN or Fermilab Tevatron colliders.

The expected top-quark signatures at $p\bar{p}$ colliders usually include a lepton from primary $t\to b\bar{l}\nu$ or $\bar{t}\to\bar{b}l\bar{\nu}$ semileptonic decay; for kinematic reasons this lepton can be more isolated from accompanying hadrons than a similar lepton from b or c decays, so lepton isolation is an important criterion for discriminating against backgrounds.[11,12] Single-lepton signals have been most commonly discussed,[10–37] but additional leptons may be present, from the $t\to b\to c\to s$ cascade decay chain or from the decay of the other quark in a $t\bar{t}$ or $W\to t\bar{b}$ pair. Both dilepton[13–15,27,28,31] and trilepton[17,29,31] signals have been discussed. The neutrinos emitted in semileptonic decays carry off missing transverse momentum ($\not{p}_T$), that can in principle be measured from the overall p_T imbalance of the other particles, and can be included in the signature. Bottom-quark jets arising in decays such as $W\to t\bar{b}$ and $t\to be\nu$ can also be exploited and provide additional signatures, especially in $W\to t\bar{b}$ events where the decay kinematics are strongly constrained.[11] If there is a microvertex detector to select events with multiple secondary decay vertices, topological signatures for the top quark can also be devised.[30]

To evaluate any one of these signatures, detailed realistic calculations of the top signal and the principal backgrounds from $b\bar{b}$, $c\bar{c}$, W, and Z production are required. Hitherto such calculations have mostly been made for energies $\sqrt{s}=540$–630 GeV appropriate to the CERN collider, where the UA1 experimental data[10] have so far disclosed no clear top signal. In the present paper, we report extensive calculations at the energy $\sqrt{s}=2000$ GeV

of the Fermilab Tevatron, which has recently come into operation and has the benefit of higher cross sections for heavy-quark production. We choose acceptance cuts appropriate to the CDF and $D0$ detectors at the Tevatron and set out to evaluate the most promising top-quark signatures based on isolated leptons, missing p_T, and jets.

Our present analysis concentrates on top-quark masses up to 100 GeV and assumes that top-quark decays are dominated by charged-current transitions $t \to bW^+$, with W either virtual or real. We thereby implicitly assume that there are no charged Higgs bosons $H^\pm$ with mass $m_H < m_t - m_b$, since in this case real $t \to bH^+$ decays would dominate[38] over virtual $t \to bW^+$ transitions (for $m_t < M_W + m_b$) and could be comparable to real $t \to bW^+$ decays (for $m_t > M_W + m_b$). This light-$H^\pm$ scenario[39] gives different top signatures,[40,41] based on missing p_T or τ jets, but may be regarded as unconventional; in contemporary superstring-inspired models[42] the charged-Higgs-boson mass is greater than 53 GeV.

II. TOP-QUARK PRODUCTION, FRAGMENTATION, AND DECAY CALCULATIONS

The lowest-order QCD subprocesses for t production are

$$q\bar{q} \to t\bar{t}, \quad gg \to t\bar{t} \ . \tag{1}$$

The total cross section for $t\bar{t}$ hadroproduction is found by folding the corresponding subprocess cross sections[43] with incident parton distributions, evolved up to an appropriate scale (which we take to be $Q^2 = \hat{s}/4$, where $\hat{s}$ is the subprocess c.m. energy squared). We use the parton distributions of Duke and Owens,[44] based on a QCD scale parameter $\Lambda = 0.2$ GeV and four active flavors.

In subprocess cross sections we use the one-loop formula

$$\alpha_s\left(\frac{\hat{s}}{4}\right) = \frac{12\pi}{(33-2f)\ln[\hat{s}/(4\Lambda_f^2)]} \ , \tag{2}$$

for the coupling α_s, where f is the number of active flavors. We assume $f=4$ with $\Lambda_4 = 0.2$ GeV up to bottom threshold at $\hat{s} = 4m_b^2$, $f=5$ in the interval $4m_b^2 < \hat{s} < 4m_t^2$ and $f=6$ for $\hat{s} > 4m_t^2$. The values of Λ_5 and Λ_6 are fixed by requiring α_s to be continuous across the bottom and top thresholds.

It has long been recognized[22-26] that QCD radiation has important effects on the dynamical distributions of produced heavy quarks, affecting the fraction of events that will survive any given acceptance cuts. We include the bulk of these effects by calculating the dynamical t and $\bar{t}$ distributions from the tree-level $2 \to 3$ QCD subprocesses:

$$q\bar{q} \to t\bar{t}g, \quad gg \to t\bar{t}g, \quad gq \to t\bar{t}q, \quad g\bar{q} \to t\bar{t}q \ . \tag{3}$$

These subprocesses correctly give the p_T dependence of $t\bar{t}$ pair production at large $p_T(t\bar{t})$. Convenient cross-section formulas have been given by Ellis and Sexton.[45] These cross sections have soft and collinear divergences at small $p_T(t\bar{t})$. These divergences should be removed in a complete calculation using well-defined regularization and normalization procedures implemented with respect to structure functions and jet formation. In the evaluation of the contribution of the $2 \to 3$ process such procedures currently pose considerable difficulty. As a phenomological expedient we remove these divergences by a procedure that is argued to approximate the exact calculation. In particular we remove them empirically by a multiplicative Gaussian cutoff factor

$$F(p_T) = 1 - \exp(-p_T^2/A^2) \tag{4}$$

with the parameter A adjusted to reproduce the correct total $t\bar{t}$ production cross section in lowest order (given by the Q^2-evolved $2 \to 2$ calculation). We find that this cutoff also preserves approximately the correct dependence on the invariant mass $m(t\bar{t})$. Typically we have $A = 8.3$ GeV for $m_t = 60$ GeV.

This use of a cutoff $2 \to 3$ calculation is essentially the truncated shower approximation described in Ref. 46. It correctly gives the total $t\bar{t}$ production, the dependence on $m(t\bar{t})$, and the dependence on $p_T(t\bar{t})$ at large p_T. The details of dependence at small $p_T(t\bar{t})$ are not necessarily correct, but these details are in any case smeared by the subsequent fragmentation and decay so that final results are not sensitive to them. This calculation also gives the leading features of associated jet production through the final g, q, or $\bar{q}$ produced along with $t\bar{t}$. We remark finally that the $2 \to 3$ parton scatterings of Eq. (3) already include both flavor excitation[43] ($gt \to gt$, $qt \to qt$, etc.) and gluon fragmentation ($g \to t\bar{t}$) subprocesses within them; Fig. 1 shows examples.

Possible enhancements of the cross section from higher-order nonleading corrections are usually represented by a multiplicative factor K. In our present calculations we assume $K=1$, because similar calculations[46] of $b\bar{b}$ and $c\bar{c}$ production with $K=1$ reproduce the observed $p\bar{p} \to \mu\bar{\mu}X$ dimuon rate.[47] Part of the nonleading corrections is of course already subsumed in the choice $Q^2 = \hat{s}/4$ and the value of Λ in Eq. (2).

Electroweak production of the top quark is calculated from $p\bar{p} \to W^\pm X$ with $W^+ \to t\bar{b}$ and $W^- \to b\bar{t}$ decays ($Z \to t\bar{t}$ is negligible). The total W cross section may be found by folding the lowest-order $q\bar{q}' \to W$ cross section with parton distributions evolved up to $Q^2 = M_W^2$. In order to incorporate leading QCD radiative effects, we calculate t production from the tree-level cross section[48] for

$$u\bar{d} \to W^+ g \to t\bar{b}g \tag{5}$$

with a Gaussian $p_T(W)$ cutoff adjusted to give the correct

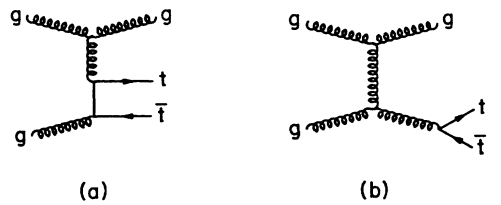

FIG. 1. Examples of $2 \to 3$ graphs that contain (a) flavor excitation and (b) gluon fragmentation subprocesses.

total cross section, following the truncated shower approximation[46] already used for $t\bar{t}$ production. The theoretical cross section through order α_s is given by the lowest-order result times a factor[49]

$$K \simeq 1+\frac{8\pi\alpha_s(M_W^2)}{9}=1.36 \ . \tag{6}$$

This gives agreement with observed $W\to l\nu$ event rates at $\sqrt{s}=630$ GeV.

Fragmentation of t quarks into top hadrons T is calculated using the model of Peterson *et al.*;[50] given the large top mass, the fragmentation function is essentially a δ function,

$$D_t^T(z)\simeq\delta(1-z) \ , \tag{7}$$

with $z=E_T/E_t$ the energy fraction. The decay of T is approximated by free-quark decay

$$t\to bxy \ , \tag{8}$$

where $xy=u\bar{d}$, $c\bar{s}$, $e^+\nu$, $\mu^+\nu$, $\tau^+\nu$ and the heavy quarks b,c fragment into B,D hadrons, respectively, according to the Peterson model (calculated in the T rest frame with parameter $\epsilon=0.5/m^2$ where m is the quark mass in GeV). We choose values $m_b=m_B=5.2$ GeV, $m_c=m_D=1.87$ GeV.

The subsequent cascade decays of B and D hadrons are also approximated by free-quark decays

$$b\to cxy, \quad c\to sxy \ . \tag{9}$$

The fragmentation of the c quark produced in B decay is known experimentally[51] to be very hard; in this particular case it appears the energy release is too small for the arguments of Ref. 50 to apply, and we describe $c\to D$ fragmentation by a δ function. The decay of produced τ leptons is represented by $\tau\to\nu xy$ matrix elements, with $xy=e\bar{\nu},\mu\bar{\nu},d\bar{u}$, using the experimental branching fraction $B_e=B_\mu=0.175$ for electron and muon modes.

In the case that $m_t>M_W+m_b$, top decay proceeds dominantly via real W bosons. Three-body decays such as $t\to be^+\nu$ then essentially factor into sequential two-body decays $t\to bW^+$, $W^+\to e^+\nu$ with strongly constrained kinematics. This provides a new source of W production[35,36] and new signatures for the top quark. We assume the W mass to be

$$M_W=81 \text{ GeV} \ , \tag{10}$$

consistent with standard-model expectations for $\sin^2\theta_W=0.23$ and with present experimental data.[52] We assume the width to be $\Gamma_W=2.1$ GeV for $m_t>M_W-m_b$: for lighter top masses Γ_W depends on m_t.

The various gluons and light quarks emitted during the production and decay processes above, fragment into final hadrons. We do not construct such final states explicitly, but take the totality of parton four-momenta to represent the distribution of hadronic energy and momentum in the calorimeters of an experimental detector. Thus we estimate the isolation of a given lepton (quantified as the sum of hadronic transverse energy depositions in a cone around the lepton) by using the original partons. We estimate the formation of jets by grouping the light partons into clusters, starting with the parton of highest p_T, with cluster size limited in azimuth ϕ and pseudorapidity $\eta=\ln\cot(\theta/2)$ by

$$\Delta R=[(\Delta\phi)^2+(\Delta\eta)^2]^{1/2}\le 0.5 \ . \tag{11}$$

If the net vectorial p_T of such a cluster exceeds a specific threshold value (taken to be 15 GeV in this paper), it is identified as a jet. This clustering of partons mirrors the clustering of hadronic-energy depositions in calorimeter cells, used in the experimental definition of hadronic jets.

III. BACKGROUND CALCULATIONS

A major background process leading to high-p_T leptons, jets, and missing p_T is the production and semileptonic decay of $b\bar{b}$ and $c\bar{c}$ pairs via QCD. The total production cross sections for single pairs are calculated from the $2\to2$ subprocesses

$$q\bar{q},gg\to Q\bar{Q} \quad (Q=b,c) \ , \tag{12}$$

with parton distributions evolved up to $\hat{s}/4$. As in the case of the top quark, the dynamical distributions are calculated from the $2\to3$ subprocesses

$$q\bar{q},gg\to Q\bar{Q}g, \quad gq(\bar{q})\to Q\bar{Q}q(\bar{q}) \tag{13}$$

with Gaussian cutoffs in p_T $(Q\bar{Q})$ chosen to reproduce the total cross sections. We also consider the possibility of double heavy pair production via the subprocesses

$$q\bar{q},gg\to Q\bar{Q}Q'\bar{Q}' \ , \tag{14}$$

where Q and Q' can be either b or c. Precise matrix elements are not known for these subprocesses, but we approximate them by the formula

$$\sum|M(ab\to Q\bar{Q}Q'\bar{Q}')|^2=4\pi\alpha_s\sum|M(ab\to Q\bar{Q}g')|^2\times\frac{2P_{Q'g'}(z)}{s'} \ , \tag{15}$$

where $\sum$ denotes spin summation, $s'=(Q'+\bar{Q}')^2$ is the $Q'\bar{Q}'$ invariant mass squared, and

$$z=(Q'\cdot g)/[(Q'\cdot g)+(\bar{Q}'\cdot g)] \ , \tag{16}$$

$$P_{Q'g'}(z)=\tfrac{1}{2}[z^2+(1-z)^2+2m_{Q'}^2/s'] \ , \tag{17}$$

with $g=Q+\bar{Q}$, $g'=Q'+\bar{Q}'$ the four-momentum of the virtual-gluon producing $Q\bar{Q}$, $Q'\bar{Q}'$, respectively. This is essentially the leading-pole approximation discussed in Ref. 45 (applied there to relate $2\to2$ with $2\to3$ matrix elements). To use this approximation we have to evaluate the $ab\to Q\bar{Q}g$ subprocess at an off-shell value of the final gluon momentum. The formulas of Ref. 45 then give negative values for the squared matrix element in some small regions of phase space; we set the cross section to zero in these regions.

The fragmentation and decay of b and c quarks are treated as in Sec. II. Light partons produced in the production and decay processes are used directly, without explicit fragmentation, to represent the flow of hadronic energy, to calculate lepton isolation, and the formation of hadronic jets.

The other major source of lepton plus jet backgrounds is W and Z production and leptonic decay. These can be evaluated using either perturbative calculations[53] or QCD shower programs.[54,55] We evaluate the background from W+jets where $W\to e\nu$ or $\mu\nu$ via a QCD shower model—the backwards-evolution method of Ref. 55. This method gives results which agree well with data on W plus jet events from the UA1 and UA2 experiments.[56]

IV. RESULTS

A. Total top-quark production

Figure 2 shows our calculated cross sections for $p\bar{p}\to t\bar{t}$ and $p\bar{p}\to W^{\pm}\to t\bar{b},b\bar{t}$ production at $\sqrt{s}=2$ TeV, versus the mass m_t. For comparison, the b and c cross sections at this energy are calculated to be

$$\begin{aligned}
&\sigma(p\bar{p}\to c\bar{c}X)=1.9\times10^{8}\text{ pb},\\
&\sigma(p\bar{p}\to b\bar{b}X)=1.9\times10^{7}\text{ pb},\\
&\sigma(p\bar{p}\to c\bar{c}c\bar{c}X)=1.2\times10^{6}\text{ pb},\\
&\sigma(p\bar{p}\to c\bar{c}b\bar{b}X)=1.1\times10^{5}\text{ pb},\\
&\sigma(p\bar{p}\to b\bar{b}b\bar{b}X)=1.2\times10^{4}\text{ pb}.
\end{aligned}\tag{18}$$

B. Single-lepton spectra and isolation

In the CDF apparatus, muon identification is restricted to the central region. We therefore calculate muon production for the pseudorapidity range $|\eta|<0.76$. Electrons and hadrons are calculated for the range $|\eta|<3$.

Figure 3 shows the calculated cross section for producing leptons (electrons plus muons) at $\sqrt{s}=2$ TeV, versus the lepton transverse momentum $p_T(l)$; for events containing more than one lepton, the highest lepton p_T is taken. Although the disparity between the top signals and the $b\bar{b}+c\bar{c}$ backgrounds is clearly reduced by selecting high p_T, an additional lepton isolation criterion is needed to suppress these backgrounds. Lepton isolation is not expected to suppress W and Z leptonic-decay backgrounds, but these have other kinematical features that can be exploited.

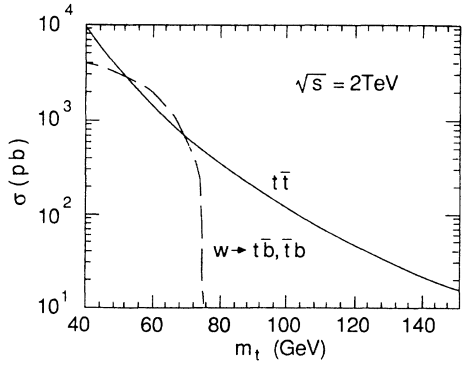

FIG. 2. Total production cross sections for $p\bar{p}\to t\bar{t}X$ and $p\bar{p}\to(t\bar{b}$ plus $\bar{t}b)X$ vs the top-quark mass at $\sqrt{s}=2$ TeV. These values can be compared with the background cross sections given in Sec. IV.

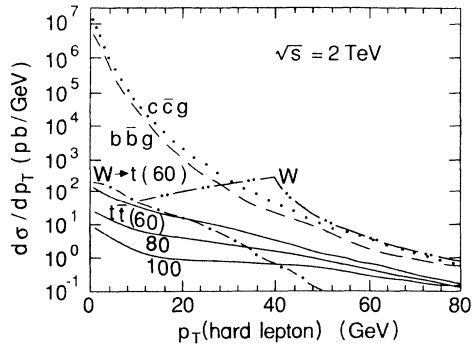

FIG. 3. The p_T spectrum of the hardest lepton in $c\bar{c},b\bar{b},W\to l\nu$, $W\to t$(60 GeV), and $t\bar{t}$ events for $m_t=60$, 80, and 100 GeV from $p\bar{p}$ collisions at $\sqrt{s}=2$ TeV.

To define lepton isolation we introduce a cone about the lepton momentum direction, given by

$$(\Delta R)^2=(\Delta\eta)^2+(\Delta\phi)^2\le(R_c)^2\ .\tag{19}$$

We define the lepton to be isolated if the sum of hadronic transverse energy $E_T=E\sin\theta$ ($=p_T$ for relativistic particles) within this cone is less than a given value E_c:

$$\sum_{\text{cone}}E_T<E_c\ .\tag{20}$$

Thus two parameters R_c and E_c specify the isolation criteria. In our present analysis we choose the values

$$R_c=0.4,\quad E_c=3\text{ GeV}\ .\tag{21}$$

We evaluate E_T by summing all the partons falling within the lepton isolation cone plus an estimate of soft contributions from the underlying event. The latter is represented by the modulus of a Gaussian random variable with mean 0 and standard deviation 1.8 GeV, following UA1 results[57] for leptons produced in W decays, rescaled to our value of R_c and the central multiplicity at $\sqrt{s}=2$ TeV.

Lepton isolation suppresses $b\bar{b}$ and $c\bar{c}$ backgrounds effectively only when $p_T(l)\gg m_b$. We therefore usually impose a lepton p_T cut:

$$p_T(l)>p_T^{\text{cut}}\ .\tag{22}$$

To illustrate the difference in isolation between top-quark signals and $b\bar{b}+c\bar{c}$ backgrounds, Fig. 4 compares the calculated distributions $d\sigma/d(\sum E_T)$ with respect to the additional transverse energy $\sum E_T$ accompanying a lepton (with $p_T^{\text{cut}}=20$ GeV) within $\Delta R=0.4$ for $p\bar{p}\to t\bar{t}X$ and $p\bar{p}\to b\bar{b}X$ processes. Very little of the $b\bar{b}$ background has $\sum E_T<3$ GeV, whereas a substantial part of the $t\bar{t}$ signal falls in this range; the tail of the distribution in the $t\bar{t}$ case is largely due to secondary semileptonic decays such as $t\to b\to cl\nu$ which are naturally nonisolated.

C. Isolated leptons plus jets

It is helpful to subdivide the isolated lepton cross section according to the number of accompanying jets. We require these jets to have

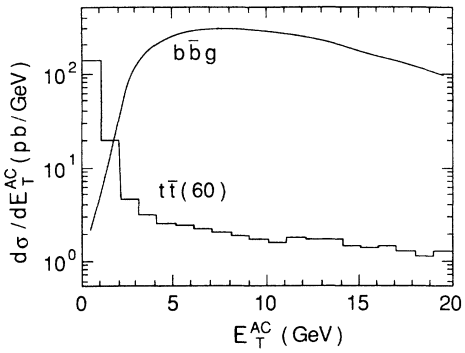

FIG. 4. Spectrum of hadronic E_T accompanying the hard lepton in a cone of $\Delta R = 0.4$ from $t\bar{t}$ events ($m_t = 60$ GeV) and $b\bar{b}$ events.

$$|\eta(\text{jet})| < 2.5, \quad p_T(\text{jet}) > 15 \text{ GeV} . \tag{23}$$

Top-quark events typically have one or more jets. Figures 5(a)–5(c) show the top signals and $b\bar{b}+c\bar{c}$ backgrounds for isolated lepton plus one, two, or three jets, plotted versus the cut on the lepton p_T. Table I lists the corresponding number of events for the 0.5 pb^{-1} integrated luminosity expected in the next run at the Tevatron collider. For the case $p_T^{\text{cut}} = 20$ GeV, the $c\bar{c}c\bar{c}$, $c\bar{c}b\bar{b}$, and $b\bar{b}b\bar{b}$ final states give negligible contributions to these cross sections. Our $b\bar{b}$ and $c\bar{c}$ background calculations are limited to $b\bar{b}x$ and $c\bar{c}x$ final states, where $x = g, q, \bar{q}$ is a light parton. For kinematical reasons these cannot contribute an isolated high-p_T lepton at the same time as three jets. Some small three-jet contributions may be expected from final states such as $b\bar{b}gg$ containing *two* light hard partons, corresponding to higher terms in the QCD shower that have not been explicitly calculated; however they would be only a small fraction of the calculated $b\bar{b}$ two-jet background and therefore negligible.

Figure 5(b) shows that in events containing two jets plus an isolated lepton having $p_{Tl} > 20$ GeV, signal exceeds $b\bar{b}$ and $c\bar{c}$ backgrounds for $m_t \lesssim 80$ GeV. The background from W production with two QCD jets is however troublesome.

Figure 5(c) shows that in $n \geq 3$ jet events with an isolated lepton the top signal exceeds all backgrounds for $m_t \lesssim 80$ GeV. For $m_t = 100$ GeV, the t signal is comparable to the background from W plus jets.

D. Missing transverse momentum

The missing transverse momentum $\not{p}_T$ is measured by the overall momentum imbalance. It contains contributions from the neutrino accompanying the isolated trigger lepton, from the neutrinos of other semileptonic decays that may be present, and from various measurement uncertainties. In our calculations we explicitly include decay neutrinos but do not fold in measurement uncertainties on $\not{p}_T$.

Figure 6 shows the calculated distribution versus $\not{p}_T$ for events containing an isolated lepton with $p_T > p_T^{\text{cut}} = 20$ GeV plus two or more jets. The $\not{p}_T$ distribution peaks at 15, 22, and 36 GeV for $m_t = 60$, 80, and 100 GeV, respectively, but the W background also introduces a strong peak.

We define as usual the "transverse mass" $m_T(l,\not{p}_T)$ of the lepton and the missing p_T, by[11,58]

$$m_T^2(l,\not{p}_T) = (|\mathbf{p}_{lT}| + |\not{\mathbf{p}}_T|)^2 - (\mathbf{p}_{lT} + \not{\mathbf{p}}_T)^2 . \tag{24}$$

Figure 7 shows the distribution versus $m_T(l,\not{p}_T)$ for events with an isolated lepton plus two or more jets. The position of the maximum is clearly correlated with m_t and offers a way to measure the top-quark mass. For $m_t < M_W$ the $m_T(e,\nu)$ distributions are approximately bounded above by m_t; when $m_t > M_W + m_b$ there is a

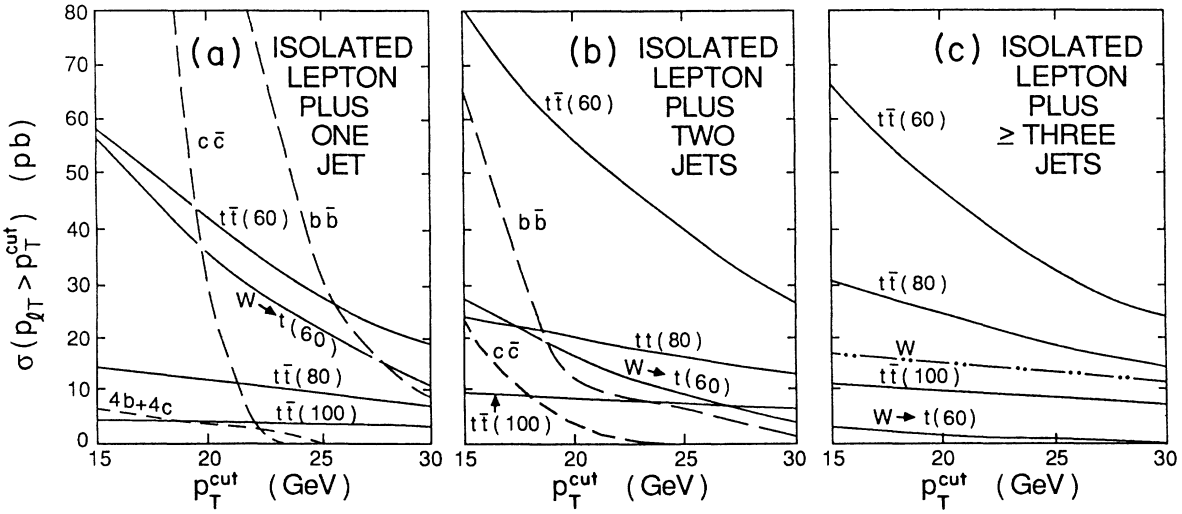

FIG. 5. Total cross sections for events containing one isolated lepton plus (a) one jet, (b) two jets, and (c) three or more jets, vs the p_T cut on the isolated lepton. The contribution from W+jets, with $W \to e$ or μ, varies from 450 to 300 pb in (a) and from 103 to 76 pb in (b).

TABLE I. Expected number of events in 1988 run of the Tevatron collider for t-quark signals ($m_t = 40$, 60, 80, and 100 GeV) and backgrounds for projected integrated luminosity 0.5 pb^{-1}. The hard isolated lepton has $p_T > 20$ GeV; other cuts are as described in the text.

Process	$l+n$ jets		ll'
	$n \geq 2$	$n \geq 3$	($m_{ll'} < 60$ GeV)
$c\bar{c}$	2	0	0
$b\bar{b}$	6	0	0
$b\bar{b}b\bar{b}$	0	0	0
$b\bar{b}c\bar{c}$	0	0	0
$c\bar{c}c\bar{c}$	0	0	0
W + jets	55	8	0
$\gamma + Z$	0	0	0.5
$Z \rightarrow \tau\bar{\tau}$	0	0	1.5
Total background	63	8	2.0
$W \rightarrow t(40)$	22	9	0
$t\bar{t}(40)$	114	34	15
$W \rightarrow t(60)$	9	1	0
$t\bar{t}(60)$	51	24	5
$t\bar{t}(80)$	22	12	2
$t\bar{t}(100)$	9	5	0.5

Jacobian peak at $m_T = M_W$ due to the decay to a real W boson.

This distribution may allow one to distinguish roughly between events containing a real W, and those containing a virtual W. For instance, requiring $m_T(l,\not{p}_T) < 60$ GeV will greatly reduce the background from real W's; the signal to background from t quarks with $m_t < 60$ GeV which decay via the three-body mode would be enhanced.

E. t-quark mass determination

In order to extract the top-quark mass from data, the information from $\not{p}_T$ and $m_T(l,\not{p}_T)$ distributions above may be supplemented by the study of other dynamical distributions. We concentrate attention now on events containing an isolated lepton plus two or more jets. Figure 8(a) shows the distribution versus invariant mass of the two hardest jets (those with highest p_T). For

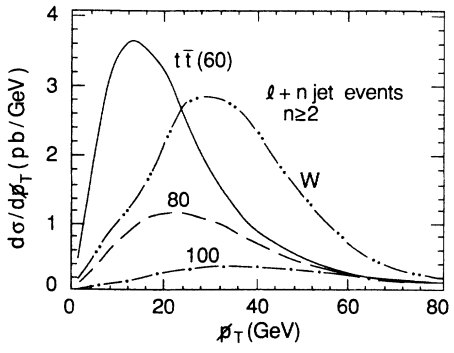

FIG. 6. Spectrum of missing transverse momentum in events with an isolated lepton with $p_T > 20$ GeV and two or more jets. We illustrate curves for $m_t = 60$, 80, and 100 GeV. The contribution from W + jets where $W \rightarrow e$ or μ is labeled W.

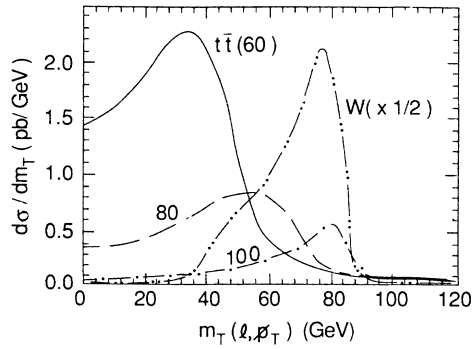

FIG. 7. Spectrum of transverse mass of the lepton mass $\not{p}_T$ in events with an isolated lepton plus two or more jets.

$m_t > M_W + m_b$, the hadronic decay $W \rightarrow q\bar{q}'$ of the W from the second top quark (assuming the first decays semileptonically) gives a dijet of mass M_W that dominates the m_{jj} distribution. This peak stands out above background from W plus jets events, allowing one to distinguish a signal above background for a t quark of mass 100 GeV. Thus, a scatter plot of $m_T(l,\not{p}_T)$ vs m_{jj} should contain events on each axis clustered about M_W if a $t \rightarrow W$ signal is to be claimed.

If we restrict attention to events with an isolated lepton plus three or more jets, then the signal to background is greatly enhanced. Figure 8(b) shows the distribution of invariant mass of the three hardest jets. A certain frac-

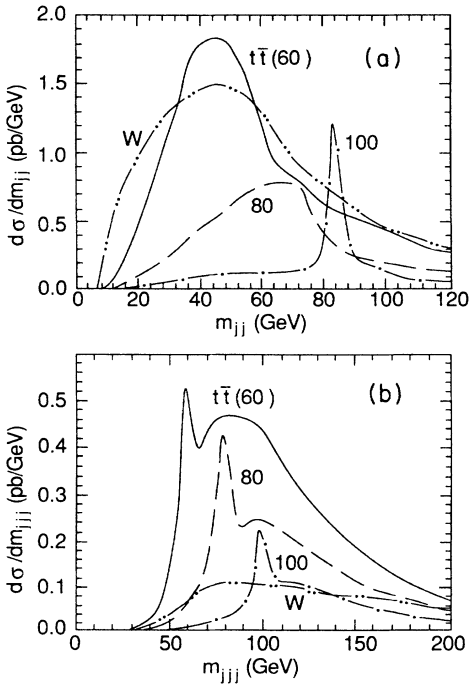

FIG. 8. Spectrum of (a) invariant mass of the two highest-p_T jets and (b) invariant mass of the three highest-p_T jets in events with an isolated lepton plus two or more jets, where the isolated lepton has $p_T > 20$ GeV. We illustrate curves for $m_t = 60$, 80, and 100 GeV. The contribution from W + jets, with $W \rightarrow e$ or μ, is labeled W.

tion of the time, these three jets all come from the same t quark, giving rise to a sharp peak at m_t which should be clear above background given adequate detector resolution of jet momentum and energy.

We may also define a "cluster transverse mass,"[11] where the lepton $|\mathbf{p}_{lT}|$ and $\mathbf{p}_{lT}$ appearing in Eq. (24) are replaced by $(|\mathbf{p}_{cT}|^2+m_c^2)^{1/2}$ and $\mathbf{p}_{cT}$ for a cluster of particles c. Figure 9 shows the distribution versus transverse mass for the cluster $(l+j_3)$, where j_3 is the third-hardest jet in events with three or more jets, combined with missing p_T. The distribution has a clear maximum, correlated with m_t. Unfortunately, for the case $m_t=100$ GeV, the distribution in this variable is very similar to the background from $W+3$ jets.

Transverse-mass variables are invariant under longitudinal boosts and insensitive to transverse boosts (unlike $\not{p}_T$). The UA1 group has proposed[10] a similar "invariant mass" quantity, where the $\not{p}_T$ transverse vector is extrapolated into a four-vector by adding a zero longitudinal momentum component and postulating $(\not{p})^2=0$, as appropriate for a neutrino. In this way a pseudoinvariant mass of lepton l, "missing energy momentum" $\not{p}$, and various jets can be constructed, although this prescription is not invariant under longitudinal boosts. Roy[37] has advocated the pseudoinvariant mass $m(l+j_2+\not{p})$ of isolated lepton plus second-hardest jet plus missing energy momentum in two-jet events; Fig. 10 shows the distribution versus this variable. It is less sharply peaked than the transverse-mass distributions in Fig. 9.

F. Dilepton events

It is interesting also to consider dilepton signals. We require both leptons to be isolated, according to our criteria above, and initially require both leptons to have $p_T>10$ GeV. Figure 11 shows how the cross sections vary if we require one of the leptons to exceed a variable cut, p_T (hard lepton) $>p_T^{\rm cut}$.

Figure 12(a) shows the invariant-mass distribution of the isolated lepton pair; Fig. 12(b) shows the azimuthal opening angle between them. Although the invariant mass contains little information about the top mass, the azimuthal correlation is more strongly back to back for lighter m_t.

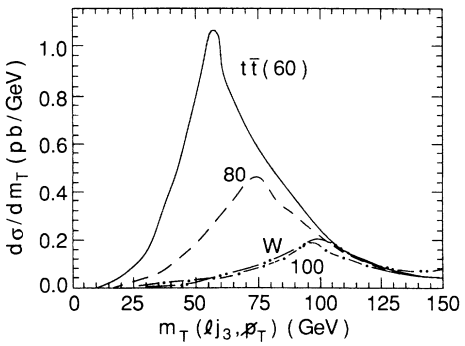

FIG. 9. Spectrum of transverse mass of the isolated lepton plus third hardest jet cluster, with $\not{p}_T$, in events containing an isolated lepton with $p_T>20$ GeV and three jets or more jets.

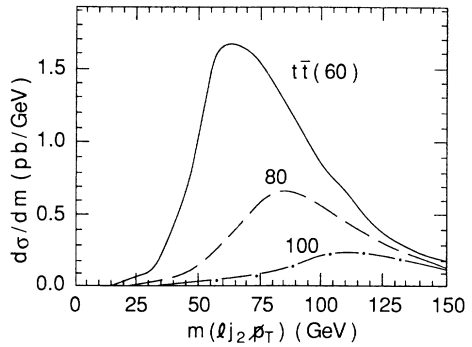

FIG. 10. Spectrum of pseudoinvariant mass of the isolated lepton plus second hardest jet plus missing p_T vector in events with one isolated lepton plus two or more jets, where $p_{lT}>20$ GeV.

These events can be either $e\bar{e}$, $\mu\bar{\mu}$, $e\bar{\mu}$, or $\mu\bar{e}$. Almost always the isolated leptons come from the primary t decays, so there should be no "two-isolated like-sign dilepton" events observable. The dominant background is γ^*, $Z\to l\bar{l}$ which is plotted in Fig. 12(a). This shows that a cut of $m_{ll'}<60$ GeV or so will be required to separate signal from background, except for the mixed flavor $e\bar{\mu}$ or $\bar{e}\mu$ events. The process $Z\to\tau\bar{\tau}$ with τ-semileptonic decays contributes a background to these events. For $m_t<80$ GeV the signal exceeds this background; see Table I. Table I gives event rates with this cut. The t-quark-initiated dilepton events will be accompanied by two b jets, and substantial $\not{p}_T$. The $\not{p}_T$ distributions from these dileptons are similar but slightly harder than the corresponding distributions of Fig. 6.

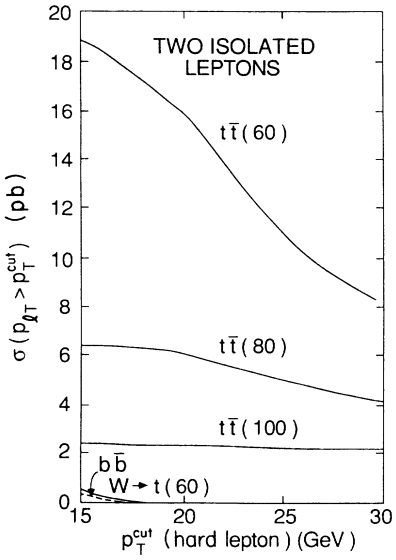

FIG. 11. Expected cross sections for events containing two isolated leptons vs the p_T cut on the hard lepton. The soft lepton has $p_T>10$ GeV. The top-quark signal is shown; we found no substantial background from other heavy flavors. The background from γ to $Z\to l\bar{l}$ where $l=e$ or μ is 216 pb for $p_T^{\rm cut}=20$ GeV.

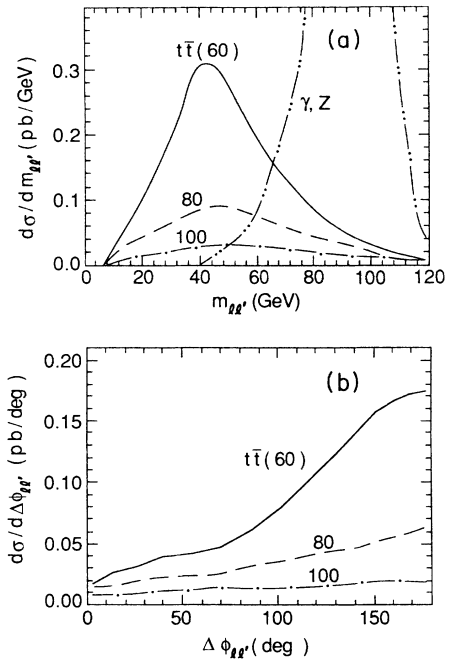

FIG. 12. Spectrum of (a) invariant mass of the two isolated leptons and (b) the transverse opening angle between the two isolated leptons in events with two isolated leptons, with p_T(hard) > 20 GeV and p_T(soft) > 10 GeV, for $m_t = 60$, 80, and 100 GeV. Also shown in (a) is the contribution from γ or $Z \rightarrow l\bar{l}$ where $l = e$ or μ.

G. Summary

We have the following.

(i) We expect the next run of the Tevatron $p\bar{p}$ collider to be able to probe up to t-quark masses of about $m_t = 100$ GeV.

(ii) The dominant identifiable signals will be isolated high-p_T leptons accompanied by two or more jets.

(iii) Differences in kinematic distributions should allow separation of t-quark signals from backgrounds from heavy flavors and vector bosons.

(iv) For $m_t < M_W$, the t mass may be obtained from the distributions in transverse mass $m_T(l,\not{p}_T)$, cluster transverse mass $m_T(l+j_3,\not{p}_T)$, and the invariant mass of the three hardest jets.

(v) For $m_t \approx 100$ GeV, the background from directly produced W plus jets poses difficulties, but the top quark can be found and its mass can be measured from the three-hard-jet invariant mass, given sufficient detector resolution.

(vi) There should be a smaller signal from events containing two isolated high-p_T leptons plus missing energy plus jets which can be used to confirm the presence of a top signal for $m_t < 80$ GeV.

Note added. After this paper was completed we received a report by P. Nason, S. Dawson, and R. K. Ellis [Report No. Fermilab-PUB-87/222-T (unpublished)] where the K factor relating the $O(\alpha_s)$ total heavy-quark cross section to the lowest-order cross section is evaluated versus the heavy-quark mass. For b quarks they find $K = 2.5$ and for t quarks $K = 1.7-1.4$ for $m_t = 40-100$ GeV, at $\sqrt{s} = 1.8$ TeV with $Q^2 = \hat{s}$. These results would not appreciably modify our conclusions; our choice of $Q^2 = \hat{s}/4$ rather than $Q^2 = \hat{s}$ increases the t-quark cross section by about 30% (equivalent to a factor $K = 1.3$) for $m_t = 80$ GeV but affects b-quark production much less.

ACKNOWLEDGMENTS

We thank L. Nodulman and J. F. Owens for discussions and J. Ohnemus for help with some of the calculations. This research was supported in part by the University of Wisconsin Research Committee with funds granted by the Wisconsin Alumni Research Foundation, in part by the U.S. Department of Energy under Contract No. DE-AC02-76ER00881, and in part by the National Science Foundation under Grant No. PHY84-14643.

[1]See, e.g., J. C. Taylor, *Gauge Theories of Weak Interactions* (Cambridge University Press, Cambridge, England, 1976).

[2]V. Barger and S. Pakvasa, Phys. Lett. **81B**, 195 (1979); G. L. Kane and M. Peskin, Nucl. Phys. **B195**, 29 (1982); A. Bean *et al.*, Phys. Rev. D **35**, 3533 (1987).

[3]W. Bartel *et al.*, Phys. Lett. **146B**, 437 (1984).

[4]U. Amaldi *et al.*, Phys. Rev. D **36**, 1385 (1987); G. Costa *et al.*, Report No. CERN-TH 4675/87 (unpublished).

[5]F. Halzen, Phys. Lett. B **182**, 388 (1986); A. D. Martin *et al.*, *ibid.* **189**, 220 (1987); V. Barger *et al.*, *ibid.* **192**, 212 (1987); F. Halzen, C. S. Kim, and S. Willenbrock, Phys. Rev. D **37**, 229 (1988); A. Datta, M. Drees, R. M. Godbole, and X. R. Tata, *ibid.* **37**, 1876 (1988).

[6]J. Ellis *et al.*, Phys. Lett. B **192**, 201 (1987); L. L. Chau and W.-Y. Keung, Davis Report No. UCD-87-02 (unpublished); I. I. Bigi and A. I. Sanda, Phys. Lett. B **194**, 307 (1987); V. Barger *et al.*, *ibid.* **194**, 312 (1987); J. R. Cudell *et al.*, *ibid.* **196**, 227 (1987); Madison Report No. MAD/PH/376 (unpublished).

[7]P. Langacker *et al.*, Phys. Rev. D **36**, 2191 (1987); A. Djouadi and C. Verzegnassi, Phys. Lett. B **195**, 265 (1987).

[8]S. Bertolini *et al.*, Phys. Rev. Lett. **59**, 180 (1987); N. G. Deshpande *et al.*, *ibid.* **59**, 183 (1987).

[9]F. Takasaki, summary of TRISTAN results presented at Hamburg Conference on Lepton and Photon Interactions, 1987 (unpublished); VENUS Collaboration, H. Yoshida *et al.*, Phys. Lett. B **198**, 570 (1987).

[10]UA1 Collaboration, Report No. CERN EP/87-190 (unpublished). For earlier data, see G. Arnison *et al.*, Phys. Lett. **147B**, 493 (1984).

[11]V. Barger *et al.*, Phys. Lett. **125B**, 339 (1983); **125B**, 343 (1983); Phys. Rev. D **28**, 145 (1983); **29**, 887 (1984); Phys. Lett. **151B**, 463 (1985).

[12]R. M. Godbole, S. Pakvasa, and D. P. Roy, Phys. Rev. Lett. **50**, 1539 (1983); D. P. Roy, Z. Phys. C **21**, 333 (1984); J. Lindfors and D. P. Roy, *ibid.* **24**, 271 (1984); R. M. Godbole and D. P. Roy, *ibid.* **29**, 83 (1985).

[13]M. Abud, R. Gatto, and C. A. Savoy, Phys. Lett. **79B**, 435

(1978).
[14]S. Pakvasa *et al.*, Phys. Rev. D **20**, 2862 (1979); F. Halzen and D. M. Scott, Phys. Lett. **129B**, 341 (1983).
[15]N. Cabibbo and L. Maiani, Phys. Lett. **87B**, 366 (1979).
[16]R. Horgan and M. Jacob, Phys. Lett. **107B**, 395 (1981); Nucl. Phys. **B238**, 221 (1984).
[17]L. L. Chau, W.-Y. Keung, and S. C. C. Ting, Phys. Rev. D **24**, 2862 (1981).
[18]F. E. Paige, in *Proton-Antiproton Collider Physics—1981*, proceedings of the Madison Workshop, edited by V. Barger, D. Cline, and F. Halzen (AIP Conf. Proc. No. 85) (AIP, New York, 1981), p. 168.
[19]K. Hagiwara and W. F. Long, Phys. Lett. **132B**, 202 (1983).
[20]G. Ballocchi and R. Odorico, Phys. Lett. **136B**, 126 (1984).
[21]B. Desai and J. Lindfors, Phys. Lett. **131B**, 217 (1983); M. Chaichian *et al.*, Phys. Rev. D **30**, 1894 (1984).
[22]V. Barger *et al.*, Phys. Rev. D **29**, 1923 (1984).
[23]L. M. Sehgal and P. Zerwas, Nucl. Phys. **B234**, 61 (1984); I. Schmitt *et al.*, Phys. Lett. **139B**, 99 (1984).
[24]R. Odorico, Nucl. Phys. **B242**, 297 (1984).
[25]F. Halzen and P. Hoyer, Phys. Lett. **154B**, 324 (1985); E. W. N. Glover *et al.*, *ibid.* **168B**, 289 (1986).
[26]A. Ali *et al.*, Nucl. Phys. **B292**, 1 (1987).
[27]V. Barger and R. J. N. Phillips, Phys. Lett. **143B**, 259 (1984); Phys. Rev. D **32**, 1128 (1985).
[28]E. W. N. Glover *et al.*, Phys. Lett. **141B**, 429 (1984).
[29]V. Barger and R. J. N. Phillips, Phys. Rev. D **30**, 1890 (1984); **34**, 2727 (1986).
[30]V. Barger and R. J. N. Phillips, Nucl. Phys. **B250**, 741 (1985).
[31]H. Baer, V. Barger, and H. Goldberg, Phys. Rev. Lett. **59**, 860 (1987).
[32]J. C. Collins, D. E. Soper, and G. Sterman, Nucl. Phys. **B263**, 37 (1987).
[33]E. L. Berger, in *Hadrons, Quarks and Gluons*, proceedings of the Twenty-second Rencontre de Moriond, Les Arcs, France, 1987, edited by J. Tran Thanh Van (Editions Frontières, Gif-sur-Yvette, 1987), p. 3.
[34]D. Atwood, A. P. Contogouris, and H. Tanaka, Phys. Rev. D **36**, 1547 (1987).
[35]S. Geer, G. Pancheri, and Y. Srivastava, Phys. Lett. B **192**, 223 (1987).
[36]P. Colas and D. Denegri, Phys. Lett. B **195**, 295 (1987).
[37]D. P. Roy, Phys. Lett. B **196**, 395 (1987).
[38]E. Golowich and T. C. Yang, Phys. Lett. **80B**, 245 (1979); D. R. T. Jones, G. L. Kane, and J. P. Leveille, Phys. Rev. D **24**, 2990 (1981); V. Barger *et al.*, *ibid.* **30**, 947 (1984), R. Raja, Report No. Fermilab-Pub-87/125-E (unpublished).
[39]S. L. Glashow and E. E. Jenkins, Phys. Lett. B **196**, 233 (1987).
[40]V. Barger and R. J. N. Phillips, Phys. Lett. B (to be published).
[41]H. Baer and X. Tata, Phys. Lett. **167B**, 241 (1986).
[42]J. F. Gunion, L. Roszkowski, and H. E. Haber, Phys. Lett. B **189**, 409 (1987); V. Barger and K. Whisnant, Madison Report No. MAD/PH/401 1987 (unpublished).
[43]See, for example, B. L. Combridge, Nucl. Phys. **B151**, 429 (1979).
[44]D. W. Duke and J. F. Owens, Phys. Rev. D **30**, 49 (1984).
[45]R. K. Ellis and J. C. Sexton, Nucl. Phys. **B282**, 642 (1987).
[46]V. Barger and R. J. N. Phillips, Phys. Rev. Lett. **55**, 2752 (1985).
[47]UA1 Collaboration, C. Albajar *et al.*, Phys. Lett. B **186**, 237 (1987).
[48]V. Barger and R. J. N. Phillips, Phys. Lett. **122B**, 83 (1983).
[49]See, e.g., V. Barger and R. J. N. Phillips, *Collider Physics* (Addison-Wesley, Reading, MA, 1987), Chap. 8.
[50]C. Peterson *et al.*, Phys. Rev. D **27**, 105 (1983).
[51]J. Green *et al.*, Phys. Rev. Lett. **51**, 347 (1983).
[52]UA1 Collaboration, G. Arnison *et al.*, Europhys. Lett. **1**, 327 (1986); UA2 Collaboration, R. Ansari *et al.*, Phys. Lett. B **186**, 440 (1987).
[53]W. J. Stirling, R. Kleiss, and S. D. Ellis, Phys. Lett. **163B**, 261 (1985); J. F. Gunion, Z. Kunszt, and M. Soldate, *ibid.* **163B**, 389 (1985).
[54]G. C. Fox and S. Wolfram, Nucl. Phys. **B168**, 285 (1980); R. Odorico, *ibid.* **B228**, 381 (1983); F. E. Paige and S. Protopopescu, Report No. BNL-37066 (unpublished); H. U. Bengtsson and T. Sjöstrand, UCLA Report No. 87-001 (unpublished).
[55]T. Gottschalk, Nucl. Phys. **B277**, 700 (1986).
[56]V. Barger, T. Gottschalk, J. Ohnemus, and R. J. N. Phillips, Phys. Rev. D **32**, 2950 (1985).
[57]UA1 Collaboration, G. Arnison *et al.*, Lett. Nuovo Cimento **44**, 1 (1985).
[58]W. L. van Neerven, J. A. M. Vermaseren, and K. J. F. Gaemers, NIKHEF Report No. H/82-20, 1982 (unpublished); UA1 Collaboration, G. Arnison *et al.*, Phys. Lett. **122B**, 103 (1983). See also J. Smith, W. L. van Neerven, and J. A. M. Vermaseren, Phys. Rev. Lett. **50**, 1738 (1983).